Sensitivity of the First Indirect Aerosol Effect to an Increase of Cloud Droplet Spectral Dispersion with Droplet Number Concentration

LEON D. ROTSTAYN

CSIRO Atmospheric Research, Aspendale, Victoria, Australia

YANGANG LIU

Brookhaven National Laboratory, Upton, New York

(Manuscript received 19 December 2002, in final form 5 May 2003)

ABSTRACT

Observations show that an increase in anthropogenic aerosols leads to concurrent increases in the cloud droplet concentration and the relative dispersion of the cloud droplet spectrum, other factors being equal. It has been suggested that the increase in effective radius resulting from increased relative dispersion may substantially negate the indirect aerosol effect, but this is usually not parameterized in global climate models (GCMs). Empirical parameterizations, designed to represent the average of this effect, as well as its lower and upper bounds, are tested in the CSIRO GCM. Compared to a control simulation, in which the relative dispersion of the cloud droplet spectrum is prescribed separately over land and ocean, inclusion of this effect reduces the magnitude of the first indirect aerosol effect by between 12% and 35%.

1. Introduction

The indirect aerosol effect is considered to be the most uncertain of the anthropogenic climate forcings that have been identified (Ramaswamy et al. 2001). It is related to an increase of cloud droplet number concentration (N) that results from an increase in the number of aerosols that act as cloud condensation nuclei (CCN), and is usually broken down into two components. The "first indirect effect" refers to the radiative impact of a decrease in cloud droplet effective radius (r_e) that is associated with increased N. A decrease in effective radius results in an increase in cloud optical depth and cloud albedo (Twomey 1977). The "second indirect effect" refers to the radiative impact of a decrease in precipitation efficiency that is associated with increased N (Albrecht 1989). This decrease in precipitation efficiency may result in an increase in cloud liquid water path and average cloud fraction.

Attempts to calculate these effects in global climate models (GCMs) have given a wide range of uncertainty, with recent estimates lying between -1.0 and -4.4 W m^{-2} for the combined first and second indirect effects in the global mean (Rotstayn 1999; Ghan et al. 2001; Jones et al. 2001; Lohmann and Feichter 2001; Menon et al. 2002; Kristjánsson 2002). However, these estimates are difficult to reconcile with the observed temperature record. For example, Knutti et al. (2002) used a climate model of reduced complexity in combination with the observed temperature record to constrain the indirect aerosol forcing to lie between 0 and -1.2 W m^{-2}. A possible explanation for this discrepancy may be that, for some reason, GCMs greatly overestimate the magnitude of the second indirect effect. This is suggested by the fact that recent empirical studies have not supported a general increase of cloud liquid water path with increased aerosol loading (Nakajima et al. 2001; Han et al. 2002; Coakley and Walsh 2002). However, even the earlier GCM-based studies that excluded the second indirect effect gave a range of -0.4 to -1.85 W m^{-2} for the first indirect effect (Penner et al. 2001). Although calculations of the type reported by Knutti et al. (2002) are subject to considerable uncertainty, it still appears that the upper part of this range is not easy to reconcile with the observed temperature record. Evidence that GCMs may tend to overestimate the first indirect aerosol effect comes from the recent study by Lohmann and Lesins (2002), who used satellite-retrieved data from the Polarization and Directionality of the Earth Reflectances (POLDER) instrument to show that their GCM overestimates the rate at which cloud droplet effective radius decreases with increasing aerosol index, a quantity that is related to the aerosol column number concentration.

It is therefore of interest to consider reasons why

Corresponding author address: Dr. Leon Rotstayn, CSIRO Atmospheric Research, PMB1, Aspendale, Victoria 3195, Australia.
E-mail: leon.rotstayn@csiro.au

GCMs may tend to overestimate the indirect aerosol effect. Existing GCM-based calculations include many simplifications and uncertainties, and cannot capture all the subtle aspects of the interaction between aerosols and clouds (Haywood and Boucher 2000). For example, recent studies have found that cloud albedo increases more slowly with aerosol loading than expected for a constant cloud liquid water content, possibly due to a combination of increased cloud absorption of shortwave radiation and enhanced evaporation of cloud droplets in polluted clouds (Ackerman et al. 2000a; Coakley and Walsh 2002). Some of the postulated interactions that lead to enhanced evaporation are complex, and are difficult to resolve with the coarse vertical resolution and simplified physics that are used in GCMs. Recently, Liu and Daum (2002) discussed another aspect of the indirect aerosol effect that has not been considered in the GCM-based studies mentioned earlier. They compiled observations that showed a systematic increase in the breadth of the cloud droplet spectrum with increasing N, due to increasing anthropogenic aerosols. The breadth is measured by the relative disperson (ϵ), defined as the ratio of the standard deviation to the mean radius of the droplet number size distribution. For a given volume-averaged mean radius, an increase in ϵ results in an increase in droplet effective radius, which is given by

$$r_e = \beta\left(\frac{3L}{4\pi\rho_l N}\right)^{1/3}, \tag{1}$$

where L is the cloud liquid water content, ρ_l is the density of liquid water, and the spectral shape factor β is well approximated by (Liu and Daum 2000a,b)

$$\beta = \frac{(1 + 2\epsilon^2)^{2/3}}{(1 + \epsilon^2)^{1/3}}. \tag{2}$$

The observations, shown previously by Liu and Daum (2002), are reproduced in simplified form in Fig. 1. They were obtained from measurements in polluted and unpolluted warm stratiform and shallow cumulus clouds southwest of San Diego (Noonkester 1984), over the northeastern Pacific (Albrecht et al. 1988; Yum and Hudson 2001), the northeastern Atlantic (Garrett and Hobbs 1995; Hudson and Li 1995; Hudson and Yum 1997; Yum and Hudson 2001), the Southern Ocean (Boers et al. 1998; Bates et al. 1998; Yum and Hudson 2001), the eastern Florida coast (Knight and Miller 1998; Hudson and Yum 2001; Yum and Hudson 2001), west of California (Ackerman et al. 2000b; Noone et al. 2000a,b) and over the northern Indian Ocean (McFarquhar and Heymsfield 2001). The spectral shape factor is an increasing function of the relative dispersion, so that, for example, an increase of ϵ from 0.3 to 0.6 gives an increase of β from 1.09 to 1.30. Liu and Daum (2002) argued that the tendency of ϵ to increase with N may substantially negate the effect of increased N on effective radius and hence on cloud albedo.

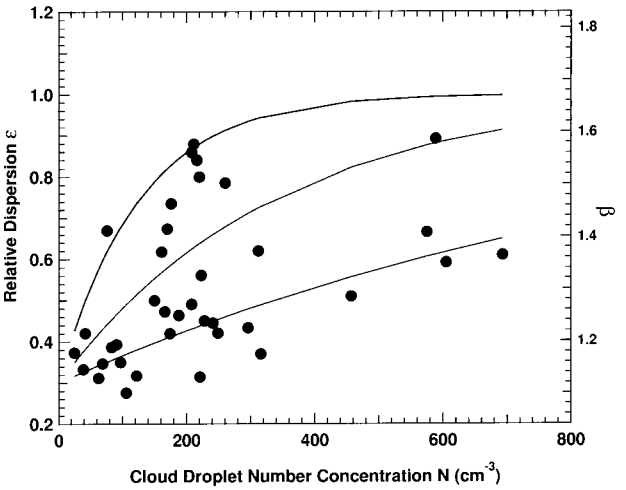

FIG. 1. Measurements of the relation between the relative dispersion of the cloud droplet spectrum (ϵ) and the cloud droplet number concentration (N). The lower, middle, and upper curves show the parameterizations used in the LOWER, MIDDLE, and UPPER simulations, respectively. Also shown on the right axis are the corresponding values of β, as given by Eq. (2).

Although there is no definite explanation at this stage for why increasing anthropogenic aerosols simultaneously increases the droplet concentration and the relative dispersion, some suggestions have been provided. Srivastava (1991) showed that the variance of the droplet spectrum increases with time if the effect of surface tension is included in the adiabatic condensational growth equation, and that the surface-tension-caused enhancement in the variance increases with the droplet concentration. According to this study, polluted clouds with a higher droplet concentration tend to have a larger relative dispersion, other factors being the same. This result was further confirmed by the numerical experiments of Wood et al. (2002) using an ensemble of adiabatic air parcels consisting of aerosols of pure ammonium sulfate. Hudson and Yum (1997) further showed, using an adiabatic cloud model, that higher total concentration (C) and lower slope (k) of the CCN power-law spectrum associated with polluted clouds leads to larger standard deviation of the droplet spectrum. Another idea was proposed by Feingold and Chuang (2002), who argued that organic films that form on the surface of haze droplets can cause increases in the relative dispersion as large as tenfold. A broader aerosol size distribution was also found to give rise to a larger relative dispersion. Therefore, the simultaneous increase of the relative dispersion and droplet concentration with increased aerosol loading may be due to a more complex chemical heterogeneity of anthropogenic aerosols, a broader size distribution, more small droplets competing for water vapor in polluted clouds compared to clean clouds, or a combination of the three (Liu and Daum 2002). Some gases in polluted clouds have also been suggested to affect cloud microphysics and gen-

erate broader droplet size distributions (Zhang et al. 1999; Charlson et al. 2001).

The purpose of this short paper is to evaluate the sensitivity of a GCM-based calculation of the first indirect effect to simple parameterizations of the increase of ϵ with N suggested by the data in Fig. 1. The model is described in section 2. Results are presented in section 3, with a summary and concluding remarks in section 4.

2. Model description

We have fitted three curves to the data in Fig. 1, designed to represent the average variation of ϵ with N, as well as lower and upper bounds of this variation. All curves are represented by equations of the form

$$\epsilon = 1 - 0.7 \exp(-\alpha N), \tag{3}$$

where $\alpha = 0.001$ for the lower curve, 0.003 for the middle curve, and 0.008 for the upper curve. It should be noted that there is considerable scatter in the data.

We have tested these simple parameterizations in a low-resolution (spectral R21) version of the Commonwealth Scientific and Industrial Research Organization (CSIRO) Mark 3 GCM (Gordon et al. 2002). The model grid has a horizontal resolution of approximately 5.6° longitude × 3.2° latitude, and 18 vertical levels. The model includes a physically based cloud scheme (Rotstayn 1997; Rotstayn et al. 2000) and an interactive treatment of the tropospheric sulfur cycle (Rotstayn and Lohmann 2002). The cloud scheme includes treatments of liquid water and ice clouds, although the parameterization considered here only affects liquid water clouds. When ice and liquid water coexist in a grid box, the simplifying assumption is made that ice and liquid water are in separate parts of the grid box. The cloud droplet concentration in liquid water clouds is parameterized as an empirical function of the sulfate mass concentration m, using a relation from Boucher and Lohmann (1995), namely,

$$N = 162 m^{0.41}, \tag{4}$$

with N in cm^{-3} and m in μg m^{-3}. (Use of a sulfate-dependent parameterization of N entails the simplifying assumption that sulfate can be used as a surrogate for all aerosols that act as cloud condensation nuclei.) The droplet effective radius is then calculated using (1), with L taken as the liquid water content at the top of each model layer, based on the idea that the shortwave fluxes are largely controlled by the effective radii at cloud top (Jones et al. 1994). This amounts to increasing r_e by a factor of $2^{1/3}$ (about 1.26) relative to the midlayer value, since L is assumed to increase linearly with height within each model layer, from zero at the bottom of the layer to twice the midlayer value at the top of the layer. The values at the top of each layer may be more appropriate than the midlayer values for comparison with satellite-retrieved effective radii, since the radiances measured by satellite tend to be generated in the upper parts of the cloud. However, this is uncertain, and it should be noted that Nakajima et al. (1991) found that their retrieved effective radii were around 10% smaller than those given by a model in which L increased linearly with height. Also, it should be noted that our method of calculating r_e is based on a physical picture that is appropriate to single-layer clouds, and it is less clear whether it is appropriate to multilayer (vertically extended) clouds. However, we have found in practice that it does tend to improve the agreement between modeled and observed values of r_e.

The optical depth of liquid water clouds is

$$\tau = \frac{3L\Delta z}{2\rho_l r_e}, \tag{5}$$

where Δz is the model layer thickness. Combined with (1), this gives the expected result that $\tau \propto N^{1/3}$ (Twomey 1977), provided that $L\Delta z$ and β are fixed. The optical depths are used to calculate the cloud reflectivities and absorptivities required by the shortwave radiation routine (Lacis and Hansen 1974), using a delta-Eddington scheme (Slingo 1989). The cloud emissivity in this version of the model does not depend on N, so it is not expected that there will be any effect on longwave radiation from variations in N, other than as a result of feedbacks that may occur.

We perform four pairs of experiments, each consisting of one run with preindustrial sulfur emissions, and one run with modern-day sulfur emissions, which correspond to the year 1985. The preindustrial emissions amount to 24 Tg S yr^{-1}, and the modern-day emissions amount to 93 Tg S yr^{-1} (Rotstayn and Lohmann 2002). The preindustrial emissions are obtained from the modern-day emissions by setting the large industrial source of sulfur dioxide to zero, and the relatively small biomass-burning source of sulfur dioxide to 10% of its modern-day value. Since the simulated cloud droplet number concentration depends only on sulfate concentration, the main differences between the droplet effective radii in the two runs are expected to occur in the industrialized regions of the Northern Hemisphere, and it is likely that the model underestimates the effect of biomass-burning aerosols on droplet effective radius.

Each experiment is run for 16 yr, of which we discard the first year as a spinup period. In all runs, sea surface temperatures (SSTs) are prescribed as monthly mean values appropriate to the present climate. The only difference between the preindustrial run and the modern-day run in each pair is in the first indirect aerosol effect, because we neglect direct aerosol radiative effects, and suppress the second indirect effect by using prescribed values of N in the calculation of autoconversion in the cloud scheme. (The prescribed values are 100 cm^{-3} over oceans, and 250 cm^{-3} over land.) We decided to suppress the second indirect effect, because of the empirical studies cited in the introduction, which cast doubt on the realism of GCM calculations of the second indirect effect.

TABLE 1. Shortwave quasi forcing due to the first indirect aerosol effect, using four different schemes to specify the relative dispersion of the cloud droplet spectrum. Quasi forcings in W m^{-2}.

	CONTROL	LOWER	MIDDLE	UPPER
Global	−1.39	−1.22	−1.17	−0.90
NH	−2.07	−1.82	−1.74	−1.42
SH	−0.72	−0.62	−0.59	−0.37

The radiative perturbation due to the first indirect aerosol effect is calculated as the difference in the net shortwave flux at the top of the atmosphere between the modern-day and preindustrial runs. Although this is not a pure radiative forcing, in the sense that the atmospheric circulation is allowed to vary between the two simulations, Rotstayn and Penner (2001) found that the difference in net irradiance between two simulations, which they termed a quasi forcing, provided a good approximation to a pure radiative forcing (in which everything other than the initially perturbation is held fixed). By focusing on the shortwave flux, we eliminate any possible longwave feedbacks. The four pairs of simulations differ in the method used to calculate β, as follows:

1) CONTROL, in which β is prescribed separately over oceans ($\beta = 1.08$) and over land ($\beta = 1.14$), based on measurements from Martin et al. (1994).
2) LOWER, in which ϵ is calculated using (3), with $\alpha = 0.001$, and β is calculated using (2).
3) MIDDLE, in which ϵ is calculated using (3), with $\alpha = 0.003$, and β is calculated using (2).
4) UPPER, in which ϵ is calculated using (3), with $\alpha = 0.008$, and β is calculated using (2).

3. Results

The results from the four pairs of experiments are summarized in Table 1. The globally averaged quasi forcing of −1.39 W m^{-2} from the pair of CONTROL simulations is within the range of −0.4 to −1.85 W m^{-2} obtained by other models for the first indirect effect (Penner et al. 2001). The magnitude of the globally averaged value is 12% smaller in the LOWER simulations, 16% smaller in the MIDDLE simulations, and 35% smaller in the UPPER simulations. The decrease is largest in the UPPER simulations, because the upper curve in Fig. 1 has the largest slope over the most relevant range of droplet concentrations. Droplet concentrations simulated by the model are mostly less than 400 cm^{-3}, even in the modern-day simulations. Introduction of the new parameterization has a relatively larger effect on the shortwave quasi forcing in the Southern Hemisphere (SH) than in the Northern Hemisphere (NH). This is because droplet concentrations are generally lower in the Southern Hemisphere, so that the shift from preindustrial to modern-day conditions in the Southern Hemisphere occurs closer to the left edge of Fig. 1, where all three curves have a steeper slope.

The effect of the new parameterization is also seen in the effective radii. The simulated values over oceans are summarized in Table 2, together with long-term satellite-retrieved values from Han et al. (1994) and Kawamoto et al. (2001). The reason for restricting the comparison to oceans is that it reduces the impact of the larger landmass in the Northern Hemisphere, and of a possible bias in the first satellite retrieval over land, where dust particles over arid regions may be misinterpreted as small cloud droplets (Han et al. 1994). Further, all the data have been restricted to the region between 45°N and 45°S, because the retrieval of Han et al. is limited to these latitudes.

Although the differences between the satellite retrievals make it difficult to draw firm conclusions, it is still of interest to compare the hemispheric contrasts in effective radius, because this contrast may be regarded as a first-order estimate of the "signature" of the indirect aerosol effect (e.g., Boucher 1995). The hemispheric contrast in effective radius is 0.82 μm in the retrieval of Han et al. (1994), but only 0.14 μm in the retrieval of Kawamoto et al. (2001), even though both are based on data from the Advanced Very High Resolution Radiometer (AVHRR). Sources of error that contribute to the uncertainty in the retrieved effective radius have been discussed by Szczodrak et al. (2001) and Harshvardhan et al. (2002). It should be noted that a recent retrieval from POLDER (Breon et al. 2002) does suggest a substantial hemispheric contrast in effective radius of about 1 μm. However, this retrieval only covers the 8-month period from November 1996 to June 1997, and may tend to exaggerate the effect, due to the omission of the major biomass-burning season (July–October) in the tropical regions of the Southern Hemisphere.

Table 2 shows that the new parameterization reduces the hemispheric contrast in effective radius over oceans by between 9% and 38% relative to the CONTROL

TABLE 2. Cloud droplet effective radii from the four modern-day simulations, and from two long-term satellite retrievals, averaged over oceans between 45°N and 45°S. Effective radii in micrometers. HAN and KAWA refer to the satellite retrievals of Han et al. (1994) and Kawamoto et al. (2001), respectively.

	CONTROL	LOWER	MIDDLE	UPPER	HAN	KAWA
Global	11.23	11.66	12.36	13.81	11.92	12.51
NH	10.86	11.33	12.09	13.58	11.47	12.44
SH	11.54	11.95	12.59	14.00	12.29	12.57
SH minus NH	0.68	0.62	0.50	0.42	0.82	0.14

simulation. In all four pairs of simulations, the hemispheric contrast in effective radius lies between the two satellite-retrieved values, so we are unable to draw any firm conclusions regarding which simulations are more realistic. This underlines the importance of further observational work to reduce the uncertainty in the satellite retrievals. The global value from the MIDDLE simulation agrees well with the satellite-retrieved values, in that it lies between the values from the two retrievals. In contrast, the modeled values are smaller than the satellite-retrieved values in the CONTROL and LOWER simulations, and larger than the satellite-retrieved values in the UPPER simulation. This provides tentative support for the use of the MIDDLE parameterization in GCMs.

4. Summary and concluding remarks

Our tests in the CSIRO GCM indicated that allowing the relative dispersion (breadth) of the cloud droplet spectrum to increase with cloud droplet number concentration as suggested by observations can decrease the magnitude of the simulated first indirect aerosol effect by between 12% and 35%. The marked sensitivity to the relation between the relative dispersion and the droplet concentration suggests the need for more research to reduce the large uncertainty involved in this relationship.

In addition to aerosols, cloud dynamics such as updraft velocity and turbulent entrainment and mixing also strongly affect both the relative dispersion and droplet concentration (Beard and Ochs 1993; Telford 1996; Hudson and Yum 1997). Therefore, just as in establishing the relationship between cloud droplet concentration and aerosol loading, the effects of cloud dynamics need to be minimized or normalized to identify the effect of aerosols on the relative dispersion, for example, by examining data with the same liquid water content. Furthermore, even the same aerosols may have different microphysical effects, if they are emitted into environments with different cloud dynamics (Feingold and Chuang 2002). Such dynamical effects are likely to be the reason for the different relationships between relative dispersion and droplet concentration tested in this work, and for the large scatter in the data presented in Fig. 1. Therefore, future research to address the effects of cloud dynamics and to statistically analyze cloud dynamics over the scale of GCM grid boxes is critical for reducing the large uncertainty in the indirect aerosol effects. It is also worth mentioning that measurements of cloud droplet size distributions, and therefore relative dispersion and droplet concentration, may suffer from instrumental uncertainties because of limitations of the Forward Scattering Spectrometer Probe (FSSP) used to measure droplet size distributions (Baumgardner and Spowart 1990).

Even more puzzling than the first indirect effect is the second indirect effect, which we deliberately excluded from this study. It is worth noting that the breadth of the cloud droplet spectrum is an important factor that determines the autoconversion rate, which is expected to increase in the presence of a few large droplets (e.g., Beard and Ochs 1993). A tendency towards broader droplet spectra in polluted air masses may substantially offset the suppression of autoconversion that typically occurs in GCMs when the autoconversion rate is allowed to respond to increased droplet concentration. This effect is generally not considered in GCMs, and is another important topic for future research.

Acknowledgments. This work was funded in part by the Australian Greenhouse Office. Yangang Liu is supported by the U.S. Department of Energy, as part of the Atmospheric Radiation Measurement Program, under Contract DE-AC02-98CH10886. The authors thank Martin Platt and the anonyomous reviewers for their constructive comments on the manuscript.

REFERENCES

Ackerman, A. S., O. B. Toon, D. E. Stevens, A. J. Heymsfield, V. Ramanathan, and E. J. Welton, 2000a: Reduction of tropical cloudiness by soot. *Science,* **288,** 1042–1047.

——, ——, J. P. Taylor, D. W. Johnson, P. V. Hobbs, and R. J. Ferek, 2000b: Effects of aerosols on cloud albedo: Evaluation of Twomey's parameterization of cloud susceptibility using measurements of ship tracks. *J. Atmos. Sci.,* **57,** 2684–2695.

Albrecht, B. A., 1989: Aerosols, cloud microphysics, and fractional cloudiness. *Science,* **245,** 1227–1230.

——, D. Randall, and S. Nicholls, 1988: Observations of marine stratocumulus during FIRE. *Bull. Amer. Meteor. Soc.,* **69,** 618–629.

Bates, T. S., B. J. Huebert, J. L. Gras, F. B. Griffiths, and P. A. Durkee, 1998: The International Global Atmospheric Chemistry (IGAC) Project's First Aerosol Characterization Experiments (ACE1): Overview. *J. Geophys. Res.,* **103,** 16 297–16 318.

Baumgardner, D., and M. Spowart, 1990: Evaluation of the forward scattering spectrometer probe. Part III: Time response and laser inhomogeneity limitations. *J. Atmos. Oceanic Technol.,* **7,** 666–672.

Beard, K. V., and H. T. Ochs III, 1993: Warm-rain initiation: An overview of microphysical mechanisms. *J. Appl. Meteor.,* **32,** 608–625.

Boers, R., J. B. Jensen, and P. B. Krummel, 1998: Microphysical and short-wave radiative structure of stratocumulus clouds over the Southern Ocean: Summer results and seasonal differences. *Quart. J. Roy. Meteor. Soc.,* **124,** 151–168.

Boucher, O., 1995: GCM estimate of the indirect aerosol forcing using satellite-retrieved cloud droplet effective radii. *J. Climate,* **8,** 1403–1409.

——, and U. Lohmann, 1995: The sulfate-CCN-cloud albedo effect. A sensitivity study with two general circulation models. *Tellus,* **47B,** 281–300.

Breon, F. M., D. Tanre, and S. Generoso, 2002: Aerosol effect on cloud droplet size monitored from satellite. *Science,* **295,** 834–838.

Charlson, R. J., J. H. Seinfeld, A. Nenes, M. Kulmala, A. Laaksonen, and M. C. Facchini, 2001: Reshaping the theory of cloud formation. *Science,* **292,** 2025–2027.

Coakley, J. J. A., and C. D. Walsh, 2002: Limits to the aerosol indirect radiative effect derived from observations of ship tracks. *J. Atmos. Sci.,* **59,** 668–680.

Feingold, G., and P. Y. Chuang, 2002: Analysis of the influence of film-forming compounds on droplet growth: Implications for

cloud microphysical processes and climate. *J. Atmos. Sci.*, **59,** 2006–2018.

Garrett, T. J., and P. V. Hobbs, 1995: Droplet spectra observed in marine stratus cloud layers. *J. Atmos. Sci.*, **52,** 2977–2984.

Ghan, S., and Coauthors, 2001: A physically based estimate of radiative forcing by anthropogenic sulfate aerosol. *J. Geophys. Res.*, **106,** 5279–5293.

Gordon, H. B., and Coauthors, 2002: The CSIRO Mk3 Climate System Model. CSIRO Atmospheric Research Tech. Paper No. 60, 134 pp. [Available online at http://www.dar.csiro.au/publications/gordon_2002a.pdf.]

Han, Q., W. B. Rossow, and A. A. Lacis, 1994: Near-global survey of effective droplet radii in liquid water clouds using ISCCP data. *J. Climate,* **7,** 465–497.

——, ——, J. Zeng, and R. Welch, 2002: Three different behaviors of liquid water path of water clouds in aerosol–cloud interactions. *J. Atmos. Sci.*, **59,** 726–735.

Harshvardhan, S. E. Schwartz, C. M. Benkovitz, and G. Guo, 2002: Aerosol influence on cloud microphysics examined by satellite measurements and chemical transport modeling. *J. Atmos. Sci.*, **59,** 714–725.

Haywood, J., and O. Boucher, 2000: Estimates of the direct and indirect radiative forcing due to tropospheric aerosols: A review. *Rev. Geophys.*, **38,** 513–543.

Hudson, J. G., and H. Li, 1995: Microphysical contrasts in Atlantic stratus. *J. Atmos. Sci.*, **52,** 3031–3040.

——, and S. S. Yum, 1997: Droplet spectral broadening in marine stratus. *J. Atmos. Sci.*, **54,** 2642–2654.

——, and ——, 2001: Maritime–continental drizzle contrasts in small cumuli. *J. Atmos. Sci.*, **58,** 915–926.

Jones, A., D. L. Roberts, and A. Slingo, 1994: A climate model study of indirect radiative forcing by anthropogenic sulphate aerosols. *Nature,* **370,** 450–453.

——, ——, M. J. Woodage, and C. E. Johnson, 2001: Indirect sulphate aerosol forcing in a climate model with an interactive sulfur cycle. *J. Geophys. Res.*, **106,** 20 293–20 310.

Kawamoto, K., T. Nakajima, and T. Y. Nakajima, 2001: A global determination of cloud microphysics with AVHRR remote sensing. *J. Climate,* **14,** 2054–2068.

Knight, C. A., and L. J. Miller, 1998: Early radar echoes from small, warm cumulus: Bragg and hydrometeor scattering. *J. Atmos. Sci.*, **55,** 2974–2992.

Knutti, R., T. F. Stocker, F. Joos, and G. K. Plattner, 2002: Constraints on radiative forcing and future climate change from observations and climate model ensembles. *Nature,* **416,** 719–723.

Kristjánsson, J. E., 2002: Studies of the aerosol indirect effect from sulfate and black carbon aerosols. *J. Geophys. Res.*, **107,** 4246, doi:10.1029/2001JD000887.

Lacis, A. A., and J. E. Hansen, 1974: A parameterization for the absorption of solar radiation in the earth's atmosphere. *J. Atmos. Sci.*, **31,** 118–133.

Liu, Y. G., and P. H. Daum, 2000a: Spectral dispersion of cloud droplet size distributions and the parameterization of cloud droplet effective radius. *Geophys. Res. Lett.*, **27,** 1903–1906.

——, and ——, 2000b: Which size distribution function to use for studies related to effective radius. *Proc. 13th Int. Conf. on Clouds and Precipitation,* Reno, NV, International Association of Meteorology and Atmospheric Sciences, 586–591.

——, and ——, 2002: Indirect warming effect from dispersion forcing. *Nature,* **419,** 580–581.

Lohmann, U., and J. Feichter, 2001: Can the direct and semi-direct aerosol effect compete with the indirect effect on a global scale? *Geophys. Res. Lett.*, **28,** 159–161.

——, and G. Lesins, 2002: Stronger constraints on the anthropogenic indirect aerosol effect. *Science,* **298,** 1012–1015.

Martin, G. M., D. W. Johnson, and A. Spice, 1994: The measurement and parameterization of effective radius of droplets in warm stratocumulus clouds. *J. Atmos. Sci.*, **51,** 1823–1842.

McFarquhar, G. M., and A. J. Heymsfield, 2001: Parameterization of INDOEX microphysical measurements and calculations of cloud susceptibility: Applications for climate studies. *J. Geophys. Res.*, **106,** 28 675–28 698.

Menon, S., J. Hansen, L. Nazarenko, and Y. Luo, 2002: Climate effects of black carbon aerosols in China and India. *Science,* **197,** 2250–2253.

Nakajima, T., M. D. King, J. D. Spinhirne, and L. F. Radke, 1991: Determination of the optical thickness and effective particle radius of clouds from reflected solar radiation measurements. Part II: Marine stratocumulus observations. *J. Atmos. Sci.*, **48,** 728–750.

——, A. Higurashi, K. Kawamoto, and J. E. Penner, 2001: A possible correlation between satellite-derived cloud and aerosol microphysical parameters. *Geophys. Res. Lett.*, **28,** 1171–1174.

Noone, K. J., and Coauthors, 2000a: A case study of ship track formation in a polluted marine boundary layer. *J. Atmos. Sci.*, **57,** 2748–2764.

——, and Coauthors, 2000b: A case study of ships forming and not forming tracks in moderately polluted clouds. *J. Atmos. Sci.*, **57,** 2729–2747.

Noonkester, V. R., 1984: Droplet spectra observed in marine stratus cloud layers. *J. Atmos. Sci.*, **41,** 829–845.

Penner, J. E., and Coauthors, 2001: Aerosols, their direct and indirect effects. *Climate Change 2001: The Scientific Basis,* J. T. Houghton, et al., Eds., Cambridge University Press, 289–348.

Ramaswamy, V., and Coauthors, 2001: Radiative forcing of climate change. *Climate Change 2001: The Scientific Basis,* J. T. Houghton, et al., Eds., Cambridge University Press, 349–416.

Rotstayn, L. D., 1997: A physically based scheme for the treatment of stratiform clouds and precipitation in large-scale models. I: Description and evaluation of the microphysical processes. *Quart. J. Roy. Meteor. Soc.*, **123,** 1227–1282.

——, 1999: Indirect forcing by anthropogenic aerosols: A global climate model calculation of the effective-radius and cloud-lifetime effects. *J. Geophys. Res.*, **104,** 9369–9380.

——, and J. E. Penner, 2001: Indirect aerosol forcing, quasi-forcing and climate response. *J. Climate,* **14,** 2960–2975.

——, and U. Lohmann, 2002: Simulation of the tropospheric sulfur cycle in a global model with a physically based cloud scheme. *J. Geophys. Res.*, **107,** 4592, doi:10.1029/2002JD002128.

——, B. F. Ryan, and J. J. Katzfey, 2000: A scheme for calculation of the liquid fraction in mixed-phase stratiform clouds in large-scale models. *Mon. Wea. Rev.*, **128,** 1070–1088.

Slingo, A., 1989: A GCM parameterization for the shortwave radiative properties of water clouds. *J. Atmos. Sci.*, **46,** 1419–1427.

Srivastava, R. C., 1991: Growth of cloud drops by condensation: Effect of surface tension on the dispersion of drop sizes. *J. Atmos. Sci.*, **48,** 1596–1605.

Szczodrak, M., P. H. Austin, and P. B. Krummel, 2001: Variability of optical depth and effective radius in marine stratocumulus clouds. *J. Atmos. Sci.*, **58,** 2912–2926.

Telford, J. W., 1996: Cloud with turbulence: The role of entrainment. *Atmos. Res.*, **40,** 261–282.

Twomey, S., 1977: The influence of pollution on the shortwave albedo of clouds. *J. Atmos. Sci.*, **34,** 1149–1152.

Wood, R., S. Irons, and P. R. Jonas, 2002: How important is the spectral ripening effect in stratiform boundary layer clouds? Studies using simple trajectory analysis. *J. Atmos. Sci.*, **59,** 2681–2693.

Yum, S. S., and J. G. Hudson, 2001: Microphysical relationships in warm clouds. *Atmos. Res.*, **57,** 81–104.

Zhang, Y. P., S. M. Kreidenweis, and G. Feingold, 1999: Stratocumulus processing of gases and cloud condensation nuclei 2. Chemistry sensitivity analysis. *J. Geophys. Res.*, **104,** 16 061–16 080.